Received: 5 September 2018 | Revised: 3 June 2019 | Accepted: 10 June 2019 | Published on: 8 July 2019

DOI: 10.1002/joc.6194

RESEARCH ARTICLE

International Journal of Climatology RMetS

High-quality sea surface temperature measurements along coast of the Bohai and Yellow Seas in China and their long-term trends during 1960–2012

Yan Li[1,2] | Lin Mu[1,3] | Qingyuan Wang[4] | Guoyu Ren[3,5] | Qinglong You[6]

[1]College of Life Sciences and Oceanography, Shenzhen University, Shenzhen, China

[2]National Marine Data and Information Service, Tianjin, China

[3]China University of Geosciences, Wuhan, China

[4]Tianjin Meteorological Observatory, Tianjin, China

[5]National Climate Center, China Meteorological Administration, Beijing, China

[6]Fudan University, Shanghai, China

Correspondence
Lin Mu, College of Life Sciences and Oceanography, Shenzhen University, Shenzhen, China.
Email: moulin1977@hotmail.com

Funding information
National Key Research and Development Program of China, Grant/Award Numbers: 2017YFC1404700, 2018YFA0605603; National Natural Science Foundation of China, Grant/Award Number: 41376014

Abstract

As semi-enclosed and shallow seas, the Bohai and Yellow Seas (hereafter, BYS) marine ecosystems are more easily affected by natural and anthropogenic climate changes than those in the open oceans. An accurate assessment of sea surface temperature (SST) change is crucial for the near-shore water environment. In this work, new high-quality monthly mean SST time series from 11 in situ coastal hydrological stations at BYS for the period of 1960–2012 have been generated. Monthly mean SST time series were initially subjected to penalized maximal *t* (PMT) test, using homogeneous monthly mean surface air temperature (SAT) series as references. Homogenized monthly mean SST series were obtained by adjusting all significant change points which have been supported by historic metadata. Our study shows that there are 29 significant change points in these 11 SST series. The majority of them are caused by instrument changes and station relocations—both account for about 51.7 and 31%, respectively. Then, homogeneous SST series are used to assess the long-term trends. As the regional average, the annual mean homogeneous SST series shows a rapid warming trend, with the rate of 0.21°C/decade. Compared to the homogeneous SST series, the original SST series underestimate the long-term trend (only 0.13°C/decade), indicating the artificial change points usually result in a warm-bias in the early period measurements. Seasonally, the most significant warming occurs in boreal winter during the period analysed. The relationships of the significant warming in boreal winter and atmospheric circulation modes have also been investigated. Results reflect the remarkable and direct influence of the East Asian Trough (EAT) on SST along the coastal BYS.

KEYWORDS

homogenization, long-term trends, penalized maximal *t* test, sea surface temperature

1 | INTRODUCTION

Global warming places shallow water ecosystems at more risk than those in the open ocean as their temperatures may change more rapidly and dramatically (Belkin, 2009; Liao *et al*., 2015; Stramska and Bialogrodzka, 2015). As semi-enclosed and shallow seas located in East Asia, the Bohai and Yellow Seas (hereafter referred to as BYS) supports much heavy shipping, fishing and oil-drilling activities. BYS has their special climate characteristics in local scale. The rapid regional warming is expected to have a large impact on marine biodiversity both at the ecosystem level

and at the population level (Giménez, 2011). Therefore, understanding the changes in sea surface temperature (SST) in the coastal ocean is much important.

Several high-quality and global gridded (typically 1 × 1°) historical SST analyses are available for large-scale basin (e.g., Rayner *et al*., 2003). The coastal waters, however, are not well represented by these data products, because of poor data coverage at the coastal areas and the coarse spatial resolutions (Li *et al*., 2017). Though satellite measurements have much higher spatial resolution, they still have some errors which can be due to the imperfect atmospheric corrections and complex coastlines (Stramska and Bialogrodzka, 2015). It is not easy to get clear and reliable conclusions on climate variability in the near-shore area. More studies are still needed, especially studies based on long-term observational SST data (Lin *et al*., 2001; Wu *et al*., 2005).

The National Marine Observation System along the coast of the China Seas has been set up and gradually improved since 1960. Among them, there are 26 coastal hydrological stations with long-term (exceeding 50 years) and continuous in situ SST measurements. However, the long-term instrumental time series are often influenced by non-climatic factors (i.e., station relocation, instrument change, and statistical methods change, etc.; see also Aguilar *et al*., 2005). These non-climatic factors can cause artificial change points (or called break points) which make the long-term data inhomogeneous and would cause certain deviation in estimating climate variability (Ren *et al*., 2005; Menne *et al*., 2010). Thus, homogenization of long-time observational data is essential for climate studies (Wan *et al*., 2010; Kuglitsch *et al*., 2012).

In China, studies currently focus on the homogenization of meteorological elements, such as surface air temperature (SAT), precipitation, sea level pressure, and so on (Li *et al*., 2004; 2012; Xu *et al*., 2013). However, we know little about the artificial change points in oceanic measurements and how these shifts affect the monitoring and detection of marine climate changes. In this paper, we first homogenized long-term SST series at 11 coastal hydrological stations at the coast of the BYS, using available metadata information and statistical homogeneity test method. Then, the homogeneous SST series were used to assess the SST change in the coastal waters at the annual and seasonal scales. Results should potentially enable us to detect the magnitude and intensity of SST warming more accurately in such semi-enclosed and shallow seas.

The remainder of this paper is structured as follows. The SST data from the coastal hydrological stations and methods for detecting and adjusting inhomogeneity are described in section 2. Section 3 presents the statistics and causes of the detected change points in the 11 SST data series. Section 4 shows the trends of SST from the homogenized SST. Possible influence of large-scale atmospheric circulation on the SST trends is presented in section 5. Conclusions and discussion are given in section 6.

2 | DATA AND METHODS

2.1 | Instrumental data and metadata

As shown in Figure 1, 11 coastal hydrological stations around BYS are selected (Table 1). In situ SST measurements are all from the coastal hydrological stations. These stations have taking routine and continuous measurements since 1960, with the percentage of missing data lower than 4%. These observed data

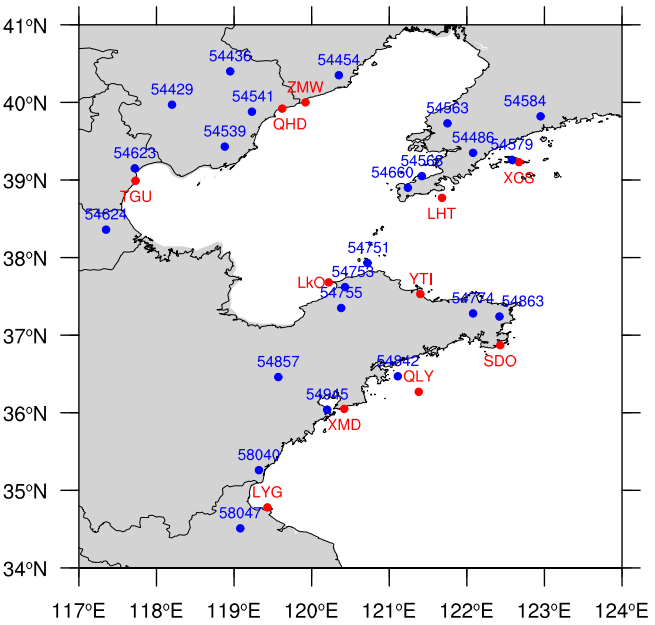

FIGURE 1 Distribution of the 11 coastal hydrological stations (red) and the reference meteorological stations (blue) [Colour figure can be viewed at wileyonlinelibrary.com]

TABLE 1 The station names and their abbreviations for each hydrological station along BYS in Figure 1

No.	Station names	Abbreviation
1	Zhi Maowan	ZMW
2	Qin Huangdao	QHD
3	Tanggu	TGU
4	Xiaochangshan	XCS
5	Laohutan	LHT
6	Longkou	LKO
7	Yantai	YTI
8	Shidao	SDO
9	Qian Liyan	QLY
10	Xiao Maidao	XMD
11	Lian Yungang	LYG

series have undergone the least relocation (no more than five relocations reported by the available metadata). All of the 11 SST series have been subjected to quality control (QC) procedures (i.e., range check, temporal and spatial consistency check, gradient check, etc.), according to the standard observation rules for China (China Standardization Administration, 2006).

Monthly mean SST was calculated from the average of each daily mean SST in a month. The monthly mean missing data were interpolated by the simple linear regression method. At first, a neighbouring reference station should be selected. For the certain month during 1960–2012, the SST series from the selected reference station was highly correlated with that from the candidate station. Then the missing value in the certain month was interpolated by the simple linear regression equation developed from the two SST series. Metadata information of the coastal hydrological stations was used to verify the statistically detected change points, including the station coordinates, height, instrument change, station relocation, environment change, algorithms for calculating a daily mean, observing procedures, observational system change, etc. All of the metadata information was documented in standard files, called "Hydrological Station History Data Files." The homogeneous monthly SAT data of meteorological stations used to build reference series were obtained from National Meteorological Information Center (NMIC) of China Meteorological Administration (CMA; Xu *et al*., 2013).

2.2 | Atmospheric circulation indices

Two atmospheric circulation indices, that is, (a) the Arctic Oscillation (AO) index and (b) the East Asian Trough (EAT) index, were used to analyse the possible connection between the large-scale atmospheric circulation and the SST variability along the coastal BYS. The two atmospheric modes (AO and EAT) drive much of the winter temperature variability across the mainland China (Chen *et al*., 2013; You *et al*., 2013; Sun *et al*., 2017) and the winter SST variability in the China Seas (Yeh and Kim, 2010; Huang *et al*., 2016; Pei *et al*., 2017).

In our study, AO index is defined as the normalized time coefficient series of the leading mode of the empirical orthogonal function (EOF1) of 1,000 hPa geopotential height anomaly field (relative to the means of 1981–2010; 20°–90°N; Thompson and Wallace, 1998), and it was extracted from the Climate Prediction Center of the National Oceanic and Atmospheric Administration (NOAA/CPC) (https://www.esrl.noaa.gov/psd/data/correlation/ao.data). We calculated the EAT index based on the definition by Sun and Li (1997). The EAT index is defined as the normalized 500 hPa geopotential height averaged over the area (25°–45°N, 110°–145°E). When AO index is positive, the polar region is in low surface pressure which locks the cold Arctic air in the polar area. On the contrary, high pressure in the polar region in negative phase allows more southwards penetration of the cool polar air into the middle latitudes (Hansen *et al*., 2010). The EAT at 500 hPa is a key factor among those related to the East Asia Winter Monsoon (EAWM). Note that in our study, when EAT index is lower than normal, EAT is deepened and strong, taking more cold air to Northwest Pacific Ocean, and vice versa. Monthly mean geopotential heights, sea level pressure, zonal and meridional winds at 1,000 hPa from the National Centers for Environmental Prediction/National Center for Atmospheric Research (NCEP/NCAR) have been used (http://www.cdc.noaa.gov) (Kalnay *et al*., 1996).

2.3 | Change point detection

Many inhomogeneity-testing techniques were adopted for countries and regions among several climate elements (e.g., Alexandersson, 1986; Solow, 1987; Vincent, 1998). A relative test based on the penalized maximal *t* (PMT) test developed by Wang *et al*. (2007) and Wang (2008) from available software RHtest V4 was used in our study (http://etccdi.pacificclimate.org/software.shtml). This software includes plots of the relevant time series and the resulting estimate of shifts and trends in the candidate series (a series to be tested and homogenized). RHtest V4 and its previous versions have been widely used (e.g., Kuglitsch *et al*., 2012; Xu *et al*., 2013). The PMT algorithm is for detection and adjustment of artificial shifts in time series of zero trend and identically Gaussian-distributed independent of first-order autoregressive [AR(1)] errors (Wang, 2008).

As explained above, the PMT algorithm needs to use a reference series to diminish the trend and periodic components that may exist in the data series (more information can be found in Wang, 2008; Wan *et al*., 2010). Generally, the homogeneous data series from surrounding stations are used to construct reference series (Wan *et al*., 2010; Xu *et al*., 2013). However, this is not appropriate for SST data. First, the coastal hydrological stations along the BYS are sparse and not evenly distributed. Second, most coastal hydrological stations have experienced an observing system transformation from artificial system to automatic system, mostly in the period of 2001–2008. In light of this, homogeneous SAT series from neighbouring meteorological observing stations are used to construct a reference series for each SST series. This approach is considered to be available for coastal areas due to the fact that the variability of SST in this region is affected mainly by the continental climate. SAT series from neighbouring meteorological stations well represent the same climatic variability as the SST in the coastal areas of China (Sun, 2006). This method has been used in some previous studies. For instance, Stephenson *et al*. (2008) systematically detected the inhomogeneity in the SAT of

Caribbean and adjacent region using SST series as references. The process in our study is detailed below.

2.3.1 | Construction of reference series

Here, the reference meteorological observing stations were selected by the following criteria:

1. The distance between the reference meteorological observing station and the candidate coastal hydrological station should be within 100 km.
2. The correlation coefficient between the annual mean original SST series and the annual mean homogeneous SAT series should be equal to or higher than 0.70. And only in this case, the reference series can represent at least 50% the variability in the candidate series (Malcher and Schönwiese, 1987; Stephenson *et al*., 2008).
3. In order to reduce the urban heat island effect on SAT series, the selected meteorological observing stations are located at rural, towns or middle-size cities, rather than big cities according to the definition of Ren *et al*. (2010).

The meteorological stations meeting the criteria are also shown in Figure 1. The homogeneous monthly SAT series which are well correlated with the candidate SST series are used to construct the reference series by correlation coefficient weighted average method (Zhu *et al*., 2015),

$$\bar{y}_i = \frac{\sum_{j=1}^{n} \rho_j^2 \times y_{ji}}{\sum_{j=1}^{n} \rho_j^2} \bar{y}_i = \frac{\sum_{j=1}^{n} \rho_j^2 \times x_{ji}}{\sum_{j=1}^{n} \rho_j^2}, \quad (1)$$

where i denotes the time, j represents the number of the reference meteorological observing station, ρ is the correlation coefficient between yearly SST series and SAT series, x is the monthly mean SAT series and $\bar{y}$ $\bar{y}_i$ is the final monthly reference SAT series for the candidate SST series.

Take XCS hydrological station as an example. Figure 2 shows the SST series from XCS hydrological station and the SAT series of the neighbouring meteorological stations which are highly correlated with the candidate SST series (the correlation coefficients are 0.77, 0.74, 0.79, all exceeding the 99% confidence level). Then monthly mean SAT series for the candidate SST from XCS hydrological station was calculated by Equation (1). The mean annual cycles of the reference SAT series and candidate SST series have been subtracted and referred to as the de-seasonalized series. Based on PMT test and the reference series, three notable change points have been detected in the monthly mean SST series (Figure 3).

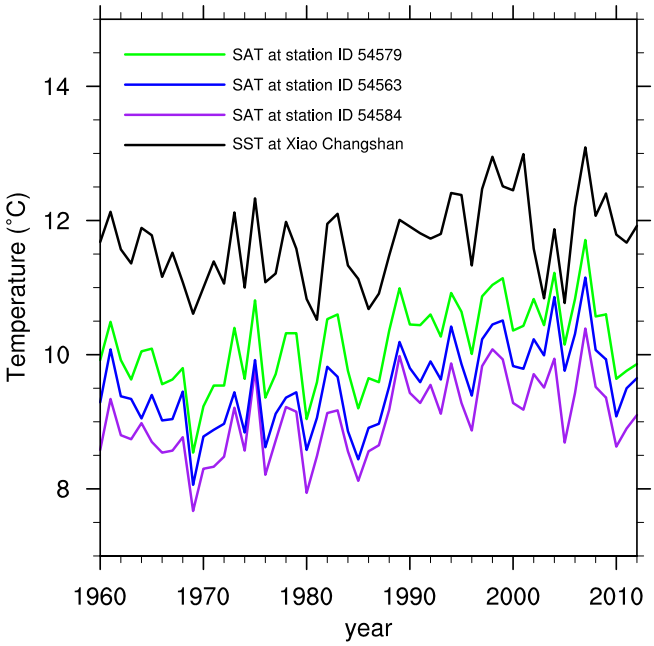

FIGURE 2 The original annual mean SST at XCS coastal hydrological station (black line) and annual mean SAT at meteorological observing stations ID 54584 (purple line), ID 54563 (blue line), and ID 54579 (green line) from 1960 to 2012 [Colour figure can be viewed at wileyonlinelibrary.com]

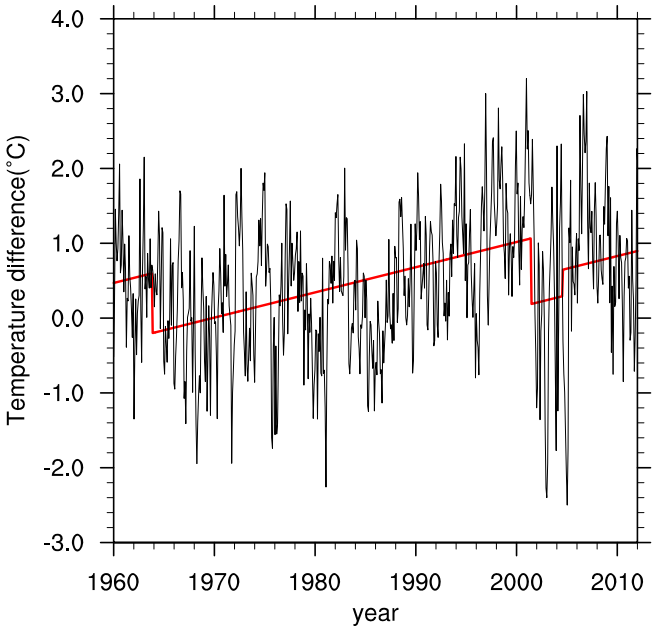

FIGURE 3 Monthly mean de-seasonalized SST series with its mean annual cycle subtracted XCS coastal hydrological station (black line). Red line: the estimated mean response along with the estimated mean shift [Colour figure can be viewed at wileyonlinelibrary.com]

2.3.2 | Verification of the change points and adjustment

In conjunction with detailed metadata of each station, these statistical change points from the PMT test were further

validated. When metadata reveal a documented change point within ±1 year of a statistical change point detected by PMT test, the statistical change point can be considered as a documented change point. In general, we retained only these documented change points for adjustment. In this case, the documented time of change is used to replace the PMT-estimated time of change for the adjustment. The change points which cannot be identified by the metadata are kept as they are, without adjustment.

As mentioned above, three change points were detected statistically in October 1964, December 2001, and January 2005 from the raw monthly mean SST series from XCS hydrological station. According to the metadata, XCS hydrological station has changed the type of thermometers for three times since 1960. The first change was on January 1, 1965. The instrument was changed from Analytic Jena 16 Mercury Thermometer to SWY1-1 Thermometer. The second change was on January 1, 2002. The observing practice was transformed from artificial observation system to automatic observation system and the instrument was changed from SWY1-1 Thermometer to YZY4-1 Thermohaline Sensor. The last change was on July 1, 2004 with transformation from YZY4-1 Thermohaline Sensor to SWL1-1 Thermometer. So the documented change points were identified as January 1965, January 2002, and July 2004. Then, we used the quantile-matching (QM) adjustment method which was combined in the RHtest V4 to adjust these shifts (Wang and Feng, 2013).

TABLE 2 The documented change points and the causes leading to inhomogeneity

			Causes of inhomogeneity		
No.	**Station**	**Documented change points**	**Station relocation**	**Change of instruments and observing system**	**Instrument fault or manual error**
1	ZMW	Nov 1967			Nov 1967
		Dec 1995			Dec 1995
		Jan 2008	Jan 2008		
		Jul 2010		Jul 2010	
2	QHD	Feb 1969			Feb 1969
		Nov 1987			Nov 1987
		Jul 2006	Jul 2006		
		Oct 2008		Oct 2008	
3	TGU	Feb 1972	Feb 1972		
		Jul 1994	Jul 1994		
		May 2002		May 2002	
4	XCS	Jan 1965		Jan 1965	
		Jan 2002		Jan 2002	
		Jul 2004		Jul 2004	
5	LHT	Feb 2002		Feb 2002	
6	LKO	Jan 1972			Jan 1972
		Jul1993	Jul 1993		
		Feb 2002		Feb 2002	
7	YTI	Feb 1974	Feb 1974		
		Sep 1980	Sep 1980		
		May 2002		May 2002	
8	SDO	May 2002		May 2002	
		Feb 2004		Feb 2004	
9	QLY	Jan 1989	Jan 1989		
		Jan 2002		Jan 2002	
10	XMD	Jan 2002		Jan 2002	
		Apr 2004		Apr 2004	
11	LYG	Jun 1983	Jun 1983		

The correlation coefficients between the homogenized annual mean SST series at XCS and three SAT series are 0.86, 0.83, and 0.86, respectively, which are higher than the original ones (0.77, 0.74, and 0.79). Comparing to the original SST series, the warming rate of the homogenized SST time series is notably larger, from 0.16 to 0.25°C/decade.

3 | STATISTICS OF DETECTED CHANGE POINTS AND CAUSES ANALYSIS

A total of 40 change points were detected at the significance level of 95% in the 11 monthly mean SST series. Among them, 29 change points are supported by the metadata (Table 2). Our analysis revealed that each SST series has experienced one or several documented change points during 1960–2012. As shown in Table 2, the instrument change and the station relocation are the main causes of change points. They are responsible for 51.7 and 31% of total documented change points, respectively. All coastal hydrological stations in BYS have experienced a transformation from artificial observing system to automatic observing system during 2001–2008. In this period, not only the types of the instrument but also the observing times each day and the calculation method of the daily mean SST were changed.

In the artificial observing period, bucket was used to sample and SST was measured by mercurial thermometer. The standard observation times were fixed at 0800, 1400, and 2000 UTC per day (China Standardization Administration, 2006). Daily mean SST was calculated by the following formula:

$$T_{\text{daily}} = (T_8 \times 2 + T_{14} + T_{20})/4.0. \quad (2)$$

In the automatic observing period, the observation instruments were installed in the thermohaline recorder wells and fixed at 0.5 m below sea level. The SST was recorded every hour per day and daily mean SST was the average of the 24-hourly observations. Previous study found that the daily/monthly mean SST in the automatic observing period was cooler than that in the artificial observing period (Yan and Li, 1997). In our study, the correction values of manual transfer were mainly between −0.20 and −0.02°C, which was in agreement with the pervious conclusions (Zhang, 1991; Hou, 2008). As reported in section 3, station relocation is another factor leading to change point. The magnitude of the relocation effects on SST is in the range of −0.9 to 0.73°C and most of the adjustments are negative. Station relocations mostly imposed an overall warming bias in SST, so that the averaged adjustment needed to diminish the effects of relocations are negative (the averaged value is −0.21°C). For each series, we adjusted the series to the most recent segment by adding ΔSST to the data before the documented change points. Finally, the homogenized monthly SST series was obtained. Statistical results detected that the larger portion (87.5%) of the ΔSST values are the negative, ranging from −0.90 to −0.01°C. The negative correction is linked tightly to the decreasing of measured SST values after automation and relocation, as mentioned above.

We made another quantitative comparison of the original and the homogenized SST series with daily NOAA OISST v2 0.25° gridded data set, which spans 1982–2012 (Banzon *et al.*, 2016). This data set is a blend of in situ and satellite measurements by the advanced very high resolution radiometer (AVHRR). Since the 11 SST series in our study were absent in OISST v2, they can be used as independent data for comparison. Daily OISST v2 was averaged into annual mean and interpolated to the observing station locations by Cressman method (Cressman, 1959). Correlation coefficients between in situ SST series (including original and homogenized series) and OISST v2 at the 11 stations are listed in Table 3. The homogenized SST time series have larger correlation coefficients than the original ones, which reflect the reliability of the homogenized SST.

4 | THE TRENDS IN ANNUAL AND SEASONAL MEAN FROM THE HOMOGENIZED DATA

Annual mean SST linear trends of the 11 coastal hydrological stations from 1960 to 2012 were calculated a simple ordinary least squares regression (Table 4). The statistical significance of the linear SST trends has been estimated by the modified Mann–Kendall trend test (Hamed and Rao, 1998; von Storch

TABLE 3 Correlation coefficients (r) between original SST, homogenized SST from the 11 coastal hydrological stations and OISSTv2 during 1982–2012

	r	
Station	**Original SST**	**Homogenized SST**
ZMW	0.66	0.71
QHD	0.74	0.80
TGU	0.78	0.87
XCS	0.68	0.74
LHT	0.85	0.90
LKO	0.76	0.80
YTI	0.83	0.88
SDO	0.78	0.79
QLY	0.93	0.94
XMD	0.82	0.82
LYG	0.89	0.91

TABLE 4 Linear trends of original and homogenized annual mean SST series of the 11 coastal hydrological stations during 1960–2012 (°C/decade)

Station	Original SST	Homogenized SST
ZMW	0.16	0.23
QHD	0.17	0.26
TGU	0.08[a]	0.13
XCS	0.16	0.25
LHT	0.20	0.22
LKO	0.15	0.24
YTI	0.09	0.15
SDO	0.14	0.17
QLY	0.14	0.18
XMD	0.20	0.22
LYG	0.15	0.21

[a]Not significant at the 95% confidence level.

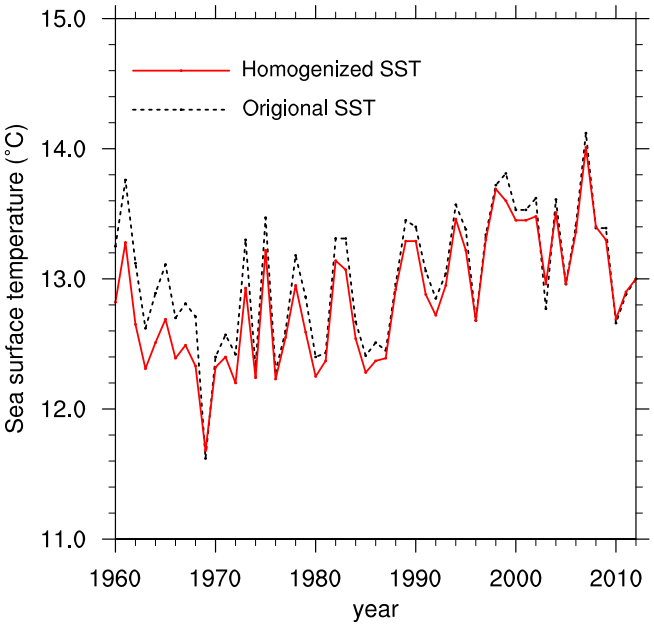

FIGURE 4 Original (black dashed line) and homogenized (red solid line) averaged annual mean of SST time series from the 11 coastal hydrological stations during 1960–2012 [Colour figure can be viewed at wileyonlinelibrary.com]

and Zwiers, 1999), with the $p < .05$ significance level. The linear trend of the averaged homogeneous SAT series along the coast of BYS is about 0.29 ± 0.07°C/decade, where the "±" indicates the 95% confidence interval. The annual mean averaged original and homogenized SST series of the total 11 stations are shown in Figure 4. The linear trend of homogenized SST series was 0.21 ± 0.06°C/decade, while the linear trend of original one is 0.13 ± 0.08°C/decade. Thus, the higher warming trend of homogenized SST time series is considered more reliable due to the fact that the homogenization adjusts the warming bias resulted from the instrument change and the station relocation. It also indicates that the SST warming rate of this region is possibly underestimated in some previous studies (Lin *et al*., 2001; Wu *et al*., 2005). Figure 5 shows the average annual mean homogenized SST anomalies and SAT anomalies from 1960 to 2012 (Figure 5a,b). Historically, after a short cooling period during 1960–1970, both of the SST and SAT in the BYE coast increased rapidly during 1970–1997, followed by a slowdown after 1998. But there was much remarkable declining tendency of SST, with the rate of −0.42°C/decade during 1998–2012. Based on the accumulated SST anomalies, we detected a significant temporal break point at 1987/1988 in the two time series from 1960 to 2012 (Figure 5c). Results indicate that there is a nearly synchronous inter-decadal transformation between the homogenized SST time series and SAT time series.

Further, in order to determine if there was a seasonality of trends in SST, we derived homogenized seasonal mean SST series. Trends in spring (MAM), summer (JJA), autumn (SON), and winter (DJF) from 1960 to 2012 are presented at each station in Figure 6. Clearly, the most significant warming rate occurred in winter (orange bars), reaching 0.30°C/decade (except TGU station) and the slowest warming trend occurred in summer (green bars), lower than 0.18°C/decade. There was an asymmetric seasonal temperature trends in the past decades. This result is consistent with previous studies of marginal sea of China based on different SST data sets (Yeh and Kim, 2010; Bao and Ren, 2014) and the SAT over the eastern mainland China (Ren *et al*., 2005).

5 | POSSIBLE CAUSES OF CONSPICUOUS SST WARMING TREND IN WINTER

Section 4 indicates that the notable warming occurred in winter along the coast of the BYS during the period of 1960–2012. The general warming may have been mainly caused by anthropogenic increase in atmospheric CO_2 concentration (WMO, 2017), and partly by the urbanization effect around the stations (Zhang *et al*., 2010). In this section, however, we further analysed the possible relationship between the warming in winter and the large-scale atmospheric circulation modes.

Figure 7 displays the Pearson's correlation coefficient between the AO index, the EAT index and the homogenized SST. We found that the winter EAT index exerted a major influence with high positive significant correlations (r_1) of 0.55–0.68 ($p < .01$) for the 11 SST series. It shows a good spatial consistency. As a moderate impact, the winter AO index was also positively and significantly correlated with winter SST, r_2 of 0.35–0.50 ($p < .01$). Figure 7 also shows the Pearson's correlation coefficient between the SST time

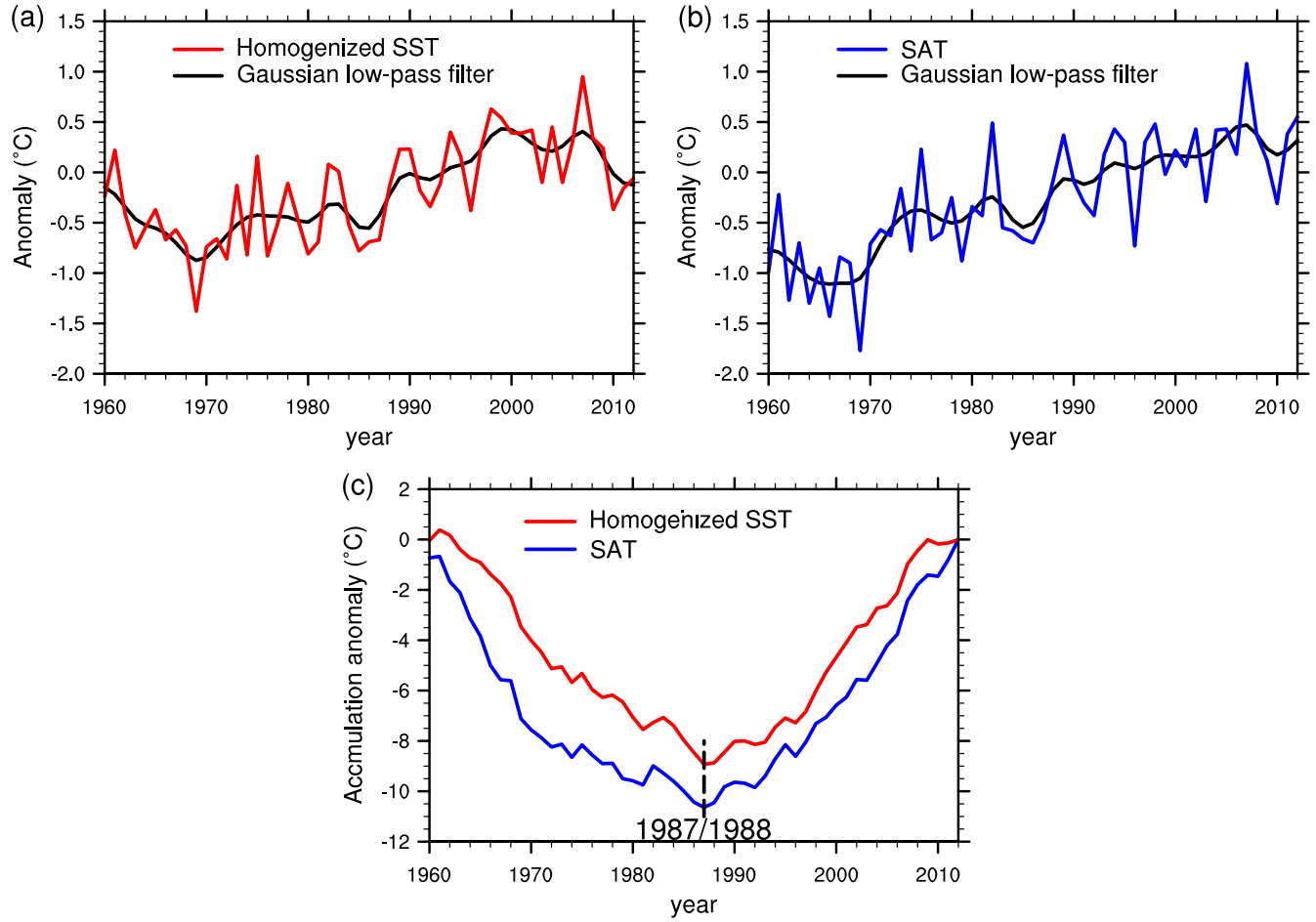

FIGURE 5 (a) Time series of regional averaged annual mean homogenized SST anomalies (red line) and its Gaussian low-pass filter (black line) for 1960–2012; (b) time series of regional averaged SAT anomalies (blue line) and its Gaussian low-pass filter (black line) for 1960–2012; (c) long-term variation of the accumulated anomalies of the region averaged annual mean homogenized SST (red line) and SAT (blue line). Black dots refer to their corresponding climate-jump years. Anomalies are departures from the 1981–2010 mean [Colour figure can be viewed at wileyonlinelibrary.com]

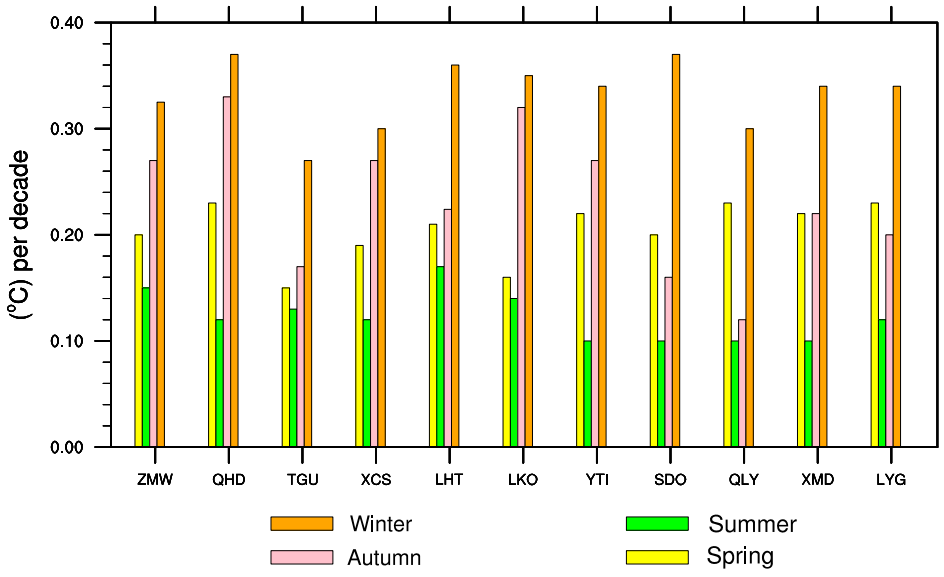

FIGURE 6 Linear trends of SST in spring (March, April, May), summer (June, July, August), autumn (September, October, November), and winter (December, January+1, February +1) for the 11 coastal hydrological stations during 1960–2012 (°C/decade) [Colour figure can be viewed at wileyonlinelibrary.com]

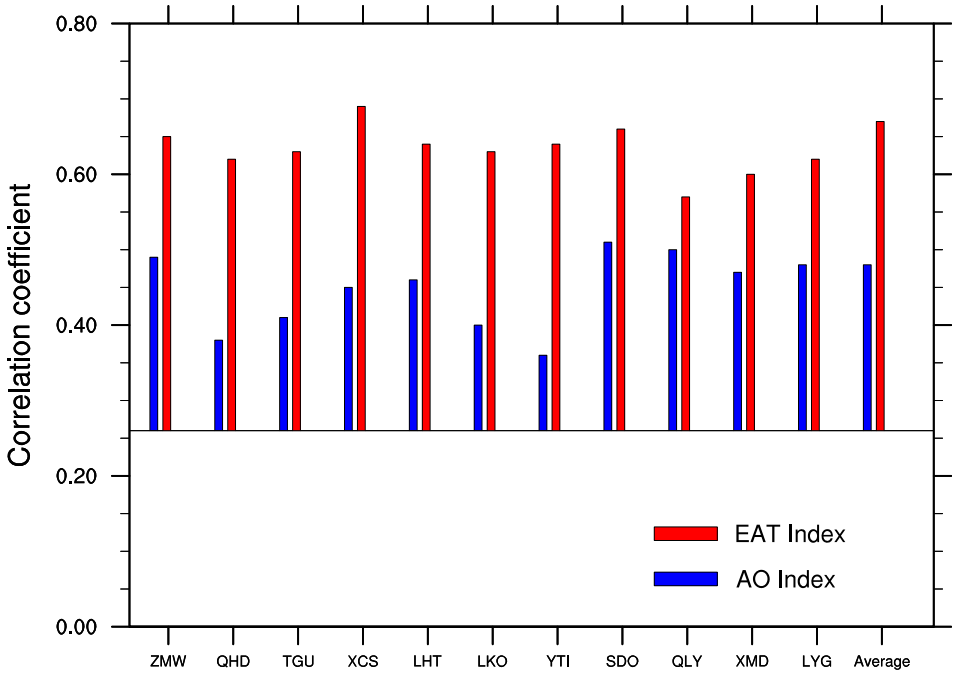

FIGURE 7 Pearson's correlation coefficient between the homogenized SST time series at 11 hydrological stations as well as the SST time series averaged across the BYE and EAT index (red bar) and AO index (blue bar) in winter 1961–2012. The reference line is 0.27 which means the 95% confidence level [Colour figure can be viewed at wileyonlinelibrary.com]

series averaged across the BYE and the two indices, with the values of 0.67 and 0.48, respectively. The result exhibits a strong relationship between the SST in this region and the two atmospheric modes in winter. Considering the significant correlation between the winter AO index and the winter EAT index (r_{12}=0.43, exceeding 95% confidence level), partial correlation analysis is applied to exclude the possible influence that is dominated by any particular event (Sankar-Rao *et al*., 1996; Ashok *et al*., 2007). Partial correlation of EAT index and SST series in each station is calculated as: $pr_1=(r_1-r_2r_{12})/\sqrt{(1-r_{12}^2)(1-r_2^2)}$. Partial correlation of the AO index and SST in each station is calculated as: $pr_2=(r_2-r_1r_{12})/\sqrt{(1-r_{12}^2)(1-r_1^2)}$. Results show that the partial correlation coefficients between the EAT index and 11 SST series are 0.41–0.62, which still exceed 95% confidence level. However, the partial correlation coefficients between the AO index and 11 SST series are 0.12–0.33, some of them are no longer significant.

To examine the change of atmosphere circulation modes, the annual and decadal mean indices of EAT and AO since 1960 are presented in Figure 8. It is notable that the winter EAT index has been consecutively increasing and transferred from negative phase (strong EAT) to positive phase (weak EAT) at 1980s. It means that the EAT has been weakening since 1960, which was confirmed by several previous studies (Wang *et al*., 2009; He, 2013). Meanwhile, the winter AO index has increased since 1960s, though decreased at 2000s (You *et al*., 2013). The spatial patterns of geopotential height at 500 hPa and wind at 1,000 hPa in winter between the first two decades (1960s and 1970s) in lower phases and the last two decades (1990s and 2000s) in higher phases (latter minus former) are presented in Figure 9a. The spatial pattern of sea level pressure in winter between the first two decades and the last two decades are presented in Figure 9b. During the strong AO index years, there is a notable annular mode over the middle-high latitudes of the Northern Hemisphere, with a significant negative SLP over the polar region (Figure 9b). Enhanced cyclonic circulation over the north of Urals (60°N, 60°E) would bring more warm airflow into northern China and the BYS, decreasing the strength of the EAT and limiting cold air southwards extension (Figure 9a). Decadal mean values of geopotential height in 2000s shows that the tilt of the EAT is larger than normal (figure omitted). These circulation abnormalities decreased the frequent bursts of winter cold waves and increased the warming at the BYS.

We further investigated the atmosphere conditions of strong AO years and weak EAT years. Weak EAT years were selected when the winter EAT indices exceeded 1.0 (i.e., 1973, 1979, 1989, 1990, 1998, 2002, 2007). Similarly, strong AO years were selected when the winter AO indices exceeded 1.0 (i.e., 1973, 1976, 1989, 1990, 1992, 1993, 2000, 2007). These years are selected to make the composite analysis next. As shown in Figure 10a, during the weak EAT years the low-level tropospheric air temperatures are positive in the most part of East China and the China Seas (exceeding 0.5°C). There are pronounced positive geopotential height anomalies located over the area (110°–150°E, 30°–40°N; Figure 10b). This atmosphere conditions are favourable to reduce the invasion of cold air from northern regions and bring warm thermal advection to the BYS. From Figure 10c, it is clear that AO significantly influences low-level tropospheric air temperature at high

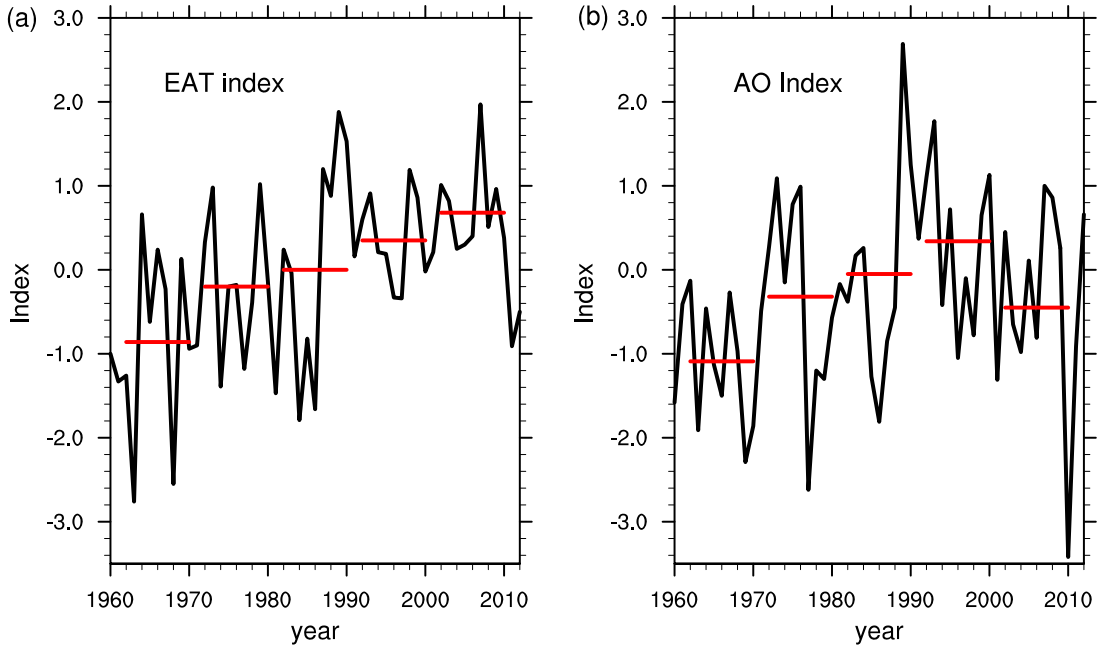

FIGURE 8 Annual (black line) and decadal mean (red line) atmospheric circulation indices of EAT (a) and AO (b) in winter 1960–2012 [Colour figure can be viewed at wileyonlinelibrary.com]

latitude of Northern Hemisphere rather than at middle latitude. However, there are remarkable negative sea level pressure anomalies around (60°–100°E, 40°–70°N). It means that in the high phase of the AO, the intensity of Siberian High (SH) is relatively weak. The positive AO can reduce the cold air from polar region and decreasing the strength of the EAWM via SH or EAT and has fewer or indirect influences on the SST along coastal BYS. EAT shows more direct and significant impacts on SST by limiting cold air southwards extension and weakening the cold wave, as well as bringing warm thermal advection at low-level tropospheric. In winter, EAT has transferred from strong phase to weak phase at 1980s. Winter SST over the BYS also switched from negative phase to positive phase at 1980s. Our study implies that robust winter SST warming in this region is closely associated with the change of EAT. The result of the composite analysis of atmospheric conditions is consistent with the result of the partial correlation analysis.

6 | CONCLUSIONS AND DISCUSSION

The SST series from the 11 coastal hydrological stations along the coast of the BYS in China have been homogenized for the period of 1960–2012 using the PMT test. Here, we proposed a novel approach for homogenizing SST using homogeneous SAT series as a reference series. Statistical change points in monthly SST series were then verified by metadata. Results show that there are totally 40 statistical change points in the 11 SST series. Among them, 29 are the documented change points and need to be adjusted. The other 11 change points which cannot be identified by the metadata are kept as they are, without adjustment. Instruments changes, including the transformation from artificial observing system to automatic observing system, and station relocations are the main causes for change points, which together accounts for 82% of discontinuities. Due to the reconstruction of ports and reclamation projects, station relocations have caused several change points in the SST series. Most of the transformations of observing system occurred during 2000–2008. All of the documented change points have been adjusted by using QM adjustment method.

Both of the homogenized and original SST series show increase in annual mean SST throughout the coast of BYS. Compared to the original SST series, all of the 11 homogeneous SST series have larger warming trends. It indicates that the effects of artificial change points or shifts on trend analysis are notable. The original SST tends to underestimate the warming trends in the study region, and the homogenized series show better consistency of trend (0.21°C/decade) with that estimated from SAT in the same region (0.29°C/decade). The reason for the difference in trend estimates between the original and homogenized series needs further study. However, the homogenization may have led to a recovery of urbanization effects in the new data series in certain extents if the stations are relocated from more urban areas to more rural areas, as documented by Zhang *et al*. (2014) for SAT data.

Furthermore, we derived seasonal mean SST series from the homogenized monthly mean series and carried out the trend analysis. Results show that there is a consistent warming in four

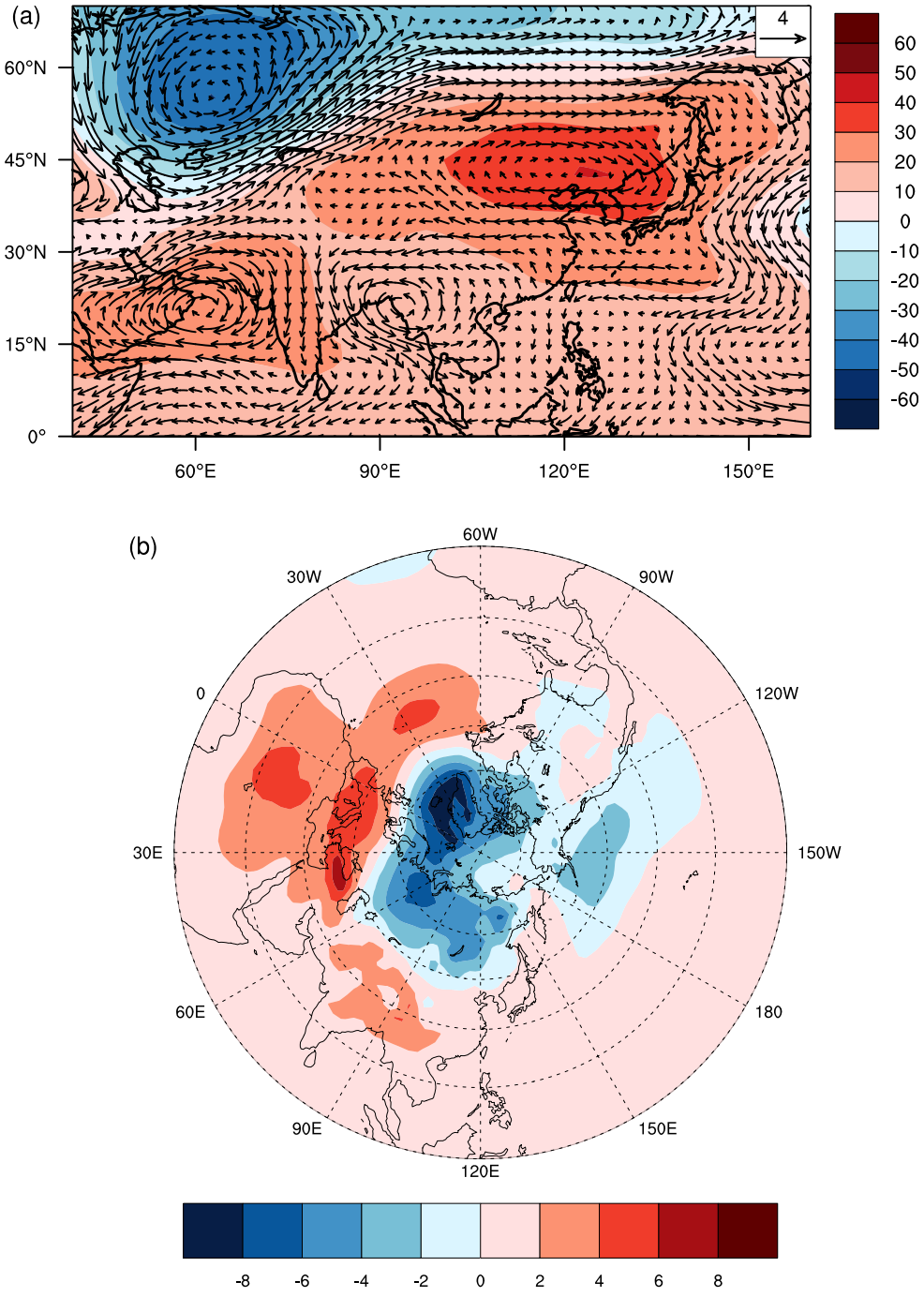

FIGURE 9 The geopotential height anomalies at 500 hPa (dagpm) and wind anomalies at 1,000 hPa (m/s) (a) and sea level pressure (b) between the last two decades (1990s and 2000s) and the first two decades (1960s and 1970s) [Colour figure can be viewed at wileyonlinelibrary.com]

seasons at the BYS coast. The largest warming rate occurs in winter, with most part exceeding 0.3°C/decade. Changes in winter climate in the Northern Hemisphere are influenced by changes in atmospheric circulation modes (You *et al*., 2011; Minola *et al*., 2016). In high phase, AO can reduce the cold air from polar region and decreasing the strength of the EAWM via SH or EAT. Meanwhile, EAT in high phase can limit cold air southwards extension and weaken the cold wave, resulting in warm thermal advection through low-level tropospheric. The BYS warming trend in winter is closely related to the abovementioned EAT and AO modes as both of them have been increasing since 1960.

Homogenization is a fundamental work for monitoring and detecting regional climate change. Based on the homogenized SST data, we confirmed the rapid warming at the BYS coast. In this study, we mainly analysed the atmospheric circulation patterns leading to climate variation of winter SST. The dynamic linkage of the decadal and trend variation of the SST with oceanic oscillation modes and local oceanic forcing, such as Pacific Decadal Oscillation (PDO) and El Niño–Southern Oscillation (ENSO) and Kuroshio Current, still needs to be investigated in future studies. Here, it should be pointed out that the possible impact of urbanization processes on the long-term trends of SST, and the contribution of the

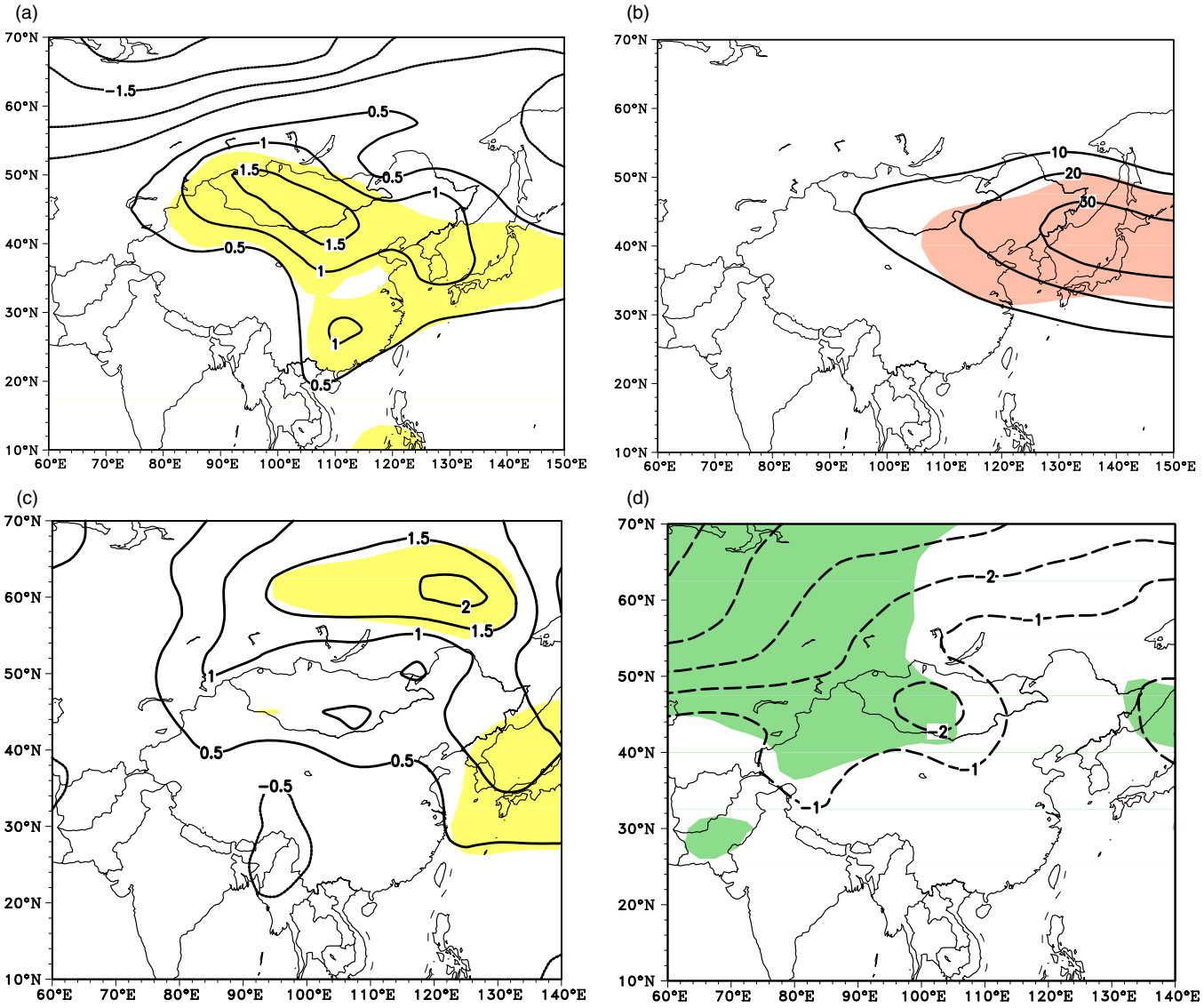

FIGURE 10 Composite winter low-level tropospheric air temperature (°C) and 500 hPa geopotential height anomalies (dagpm) in the weak phase EAT years (a, b); composite of low-level tropospheric air temperature (°C) and sea level pressure (hPa) in the high phase AO years (c, d). The shaded areas indicate the anomalies are statistically significant above the 95% confidence level based on a *t* test with (N-2) degrees of freedom [Colour figure can be viewed at wileyonlinelibrary.com]

anthropogenic global warming to the SST change in near shore areas, also need to be examined.

ACKNOWLEDGEMENTS

This study was supported by the National Key Research and Development Program of China (Grant 2017YFC1404700; Grant 2018YFA0605603) and the National Natural Science Foundation of China (Grant 41376014). The authors give many thanks to Hamburg University's Cluster of Excellence CliSAP for funding the first author's visiting in Germany in 2016 which benefits this study greatly.

ORCID

Lin Mu https://orcid.org/0000-0001-9983-6227
Guoyu Ren https://orcid.org/0000-0002-9351-4179
Qinglong You https://orcid.org/0000-0002-5329-9697

REFERENCES

Aguilar, E., Peterson, T.C., Obando, P.R., Frutos, R., Retana, J.A., Solera, M., Soley, J., González García, I., Araujo, R.M., Rosa Santos, A., Valle, V.E., Brunet, M., Aguilar, L., Álvarez, L., Bautista, M., Castañón, C., Herrera, L., Ruano, E., Sinay, J.J., Sánchez, E., Hernández Oviedo, G.I., Obed, F., Salgado, J.E., Vázquez, J.L., Baca, M., Gutiérrez, M., Centella, C., Espinosa, J.,

Martínez, D., Olmedo, B., Ojeda Espinoza, C.E., Núñez, R., Haylock, M., Benavides, H. and Mayorga, R. (2005) Changes in precipitation and temperature extremes in Central America and northern South America, 1961–2003. *Journal of Geophysical Research*, 110(D23), 1–15.

Alexandersson, H. (1986) A homogeneity test applied to precipitation data. *International Journal of Climatology*, 6(6), 661–675.

Ashok, K., Behera, S.K., Rao, S.A., Weng, H. and Yamagata, T. (2007) El Nino Modoki and its possible teleconnection. *Journal of Geophysical Research*, 112, C11007.

Banzon, V., Smith, T.M., Chin, T.M., Liu, C. and Hankins, W. (2016) A long-term record of blended satellite and in situ sea-surface temperature for climate monitoring, modeling and environmental studies. *Earth System Science Data*, 8, 165–176.

Bao, B. and Ren, G.Y. (2014) Climatological characteristics and long-term change of SST over the marginal seas of China. *Continental Shelf Research*, 77(1), 96–106.

Belkin, I.M. (2009) Rapid warming of large marine ecosystems. *Progress in Oceanography*, 81(2009), 207–213.

Chen, S.F., Chen, W. and Wei, K. (2013) Recent trends in winter temperature extremes in eastern China and their relationship with the Arctic Oscillation and ENSO. *Advances in Atmospheric Sciences*, 30(6), 1712–1724.

China Standardization Administration. (2006) *The Specification for Nearshore Observations (ICS 07.060 A 45)*. Beijing: China Standards Press, 69 pp. (in Chinese).

Cressman, G.W. (1959) An operational objective analysis system. *Monthly Weather Review*, 87(10), 367–374.

Giménez, L. (2011) Exploring mechanisms linking temperature increase and larval phenology: the importance of variance effects. *Journal of Experimental Marine Biology and Ecology*, 400(1–2), 227–235.

Hamed, K.H. and Rao, A.R. (1998) A modified Mann–Kendall trend test for autocorrelated data. *Journal of Hydrology*, 204(1–4), 182–196.

Hansen, J., Ruedy, R., Sato, M. and Lo, K. (2010) Global surface temperature change. *Reviews of Geophysics*, 48(4), 1–29.

He, S.P. (2013) Reduction of the East Asian Monsoon interannual variability after the mid-1980s and possible causes. *Chinese Science Bulletin*, 58(12), 1331–1338.

Hou, C.W. (2008) *Study on the representative of the water temperature observed by coastal observing stations of China.* Thesis, Ocean University of China, 86 pp. (in Chinese).

Huang, B.Y., Liu, C., Banzon, V.F., Zhang, H.M., Karl, T.R., Lawrimore, J.H. and Vose, R.S. (2016) Assessing the impact of satellite-based observations in sea surface temperature trends. *Geophysical Research Letters*, 43(7), 3431–3437.

Kalnay, E., Kanamitsu, M., Kistler, R., Collins, W., Deaven, D., Gandin, L., Iredell, M., Saha, S., White, G., Woollen, J., Zhu, Y., Leetmaa, A., Reynolds, R., Chelliah, M., Ebisuzaki, W., Higgins, W., Janowiak, J., Mo, K.C., Ropelewski, C., Wang, J., Jenne, R. and Joseph, D. (1996) The NCEP/NCAR 40-Year Reanalysis Project. *Bulletin of the American Meteorological Society*, 77(3), 437–471.

Kuglitsch, F.G., Auchmann, R., Bleisch, R., Bronnimann, S., Martius, O. and Stewart, M. (2012) Break detection of annual Swiss temperature series. *Journal of Geophysical Research*, 117, D13105.

Li, Q.X., Liu, X.N., Zhang, H.Z., Peterson, T.C. and Easterling, D.R. (2004) Detecting and adjusting on temporal inhomogeneity in Chinese mean surface air temperature dataset. *Advances in Atmospheric Sciences*, 21(2), 260–268.

Li, Q.X., Peng, J.D. and Shen, Y. (2012) Development of China homogenized monthly precipitation dataset during 1900–2009. *Journal of Geographical Sciences*, 22(4), 579–593.

Li, Y., Mu, L., Liu, Y.L., Wang, G.S., Zhang, D.S., Li, H. and Han, X. (2017) Analysis of variability and long-term trends of sea surface temperature over the China seas derived from a newly merged regional data set. *Climate Research*, 73, 217–231.

Liao, E.H., Lu, W.F., Yan, X.H. and Kidwell, A. (2015) The coastal ocean response to the global warming acceleration and hiatus. *Scientific Reports*, 5, 1–10.

Lin, C.L., Su, J.L., Xu, B.R. and Tang, Q.S. (2001) Long-term variation of temperature and salinity of the Bohai Sea and influence on its ecosystem. *Progress in Oceanography*, 49(1), 7–19.

Malcher, J. and Schönwiese, C.-D. (1987) Homogeneity, spatial correlation and spectral variance analysis of long European and North American air temperature records. *Theoretical and Applied Climatology*, 38, 157–166.

Menne, M.J., Williams, C.N. and Palecki, M.A. (2010) On the reliability of the U.S. surface temperature record. *Journal of Geophysical Researh*, 115, D11108.

Minola, L., Azorin-Molina, C. and Chen, D.L. (2016) Homogenization and assessment of observed near-surface wind speed trends across Sweden, 1956–2013. *Journal of Climate*, 29(20), 7397–7415.

Pei, Y.H., Liu, X.H. and He, H.I. (2017) Interpreting the sea surface temperature warming trend in the Yellow Sea and East China Sea. *Science China Earth Sciences*, 60(8), 1558–1568.

Rayner, N.A., Parker, D.E., Horton, E.B., Folland, C.K., Alexander, L.V., Rowell, D.P., Kent, E.C. and Kaplan, A. (2003) Global analyses of sea surface temperature, sea ice, and night marine air temperature since the late nineteenth century. *Journal of Geophysical Research*, 108(D14), 4407.

Ren, G.Y., Guo, J., Xu, M.Z. and Liu, X.N. (2005) Climate changes of China's mainland over the past half century. *Acta Meteorologica Sinica*, 63(6), 942–956.

Ren, G.Y., Zhang, A.Y., Chu, Z.Y., Zhou, J.X., Ren, Y.Y. and Zhou, Y.Q. (2010) Principles and procedures for selecting reference surface air temperature station in China. *Meteorological Science and Technology*, 38(1), 78–85 (in Chinese with English abstract).

Sankar-Rao, M., Lau, K.M. and Yang, S. (1996) On the relationship between Eurasian snow cover and the Asian summer monsoon. *International Journal of Climatology*, 16, 605–616.

Solow, A.R. (1987) A testing for climatic change: an application of the two phase regression model. *Journal of Applied Meteorology*, 26(10), 1401–1405.

Stephenson, T.S., Goodess, C.M., Haylock, M.R., Chen, A.A. and Taylor, M.A. (2008) Detecting inhomogeneities in Caribbean and adjacent Caribbean temperature data using sea-surface temperatures. *Journal of Geophysical Research*, 113(D21), 1–17.

Stramska, M. and Bialogrodzka, J. (2015) Spatial and temporal variability of sea surface temperature in the Baltic Sea based on 32-years (1982–2013) of satellite data. *Oceanologia*, 57(2015), 223–235.

Sun, B.M. and Li, C.Y. (1997) Relationship between disturbance of East Asian trough and tropical convection activities. *Chinese Science Bulletin*, 42(5), 500–504 (in Chinese).

Sun, X.B., Ren, G.Y., Ren, Y.Y., Fang, Y.H., Liu, Y.L., Xue, X.Y. and Zhang, P.F. (2017) A remarkable climate warming hiatus over

northeast China since 1998. *Theoretical and Applied Climatology*, 9, 1–16.

Sun, X.P. (2006) *China Offshore Area*. Beijing: China Ocean Press, pp. 201–228 (in Chinese).

Thompson, D.W.J. and Wallace, M.J. (1998) The Arctic Oscillation signature in the wintertime geopotential height and temperature fields. *Geophysical Research Letters*, 25(9), 1297–1300.

Vincent, L. (1998) A technique for the identification of in homogeneities in Canadian temperature series. *Journal of Climate*, 11, 1094–1104.

von Storch, H. and Zwiers, F.W. (1999) *Statistical Analysis in Climate Research*. London: Cambridge University Press.

Wan, H., Wang, X.L. and Swail, V.R. (2010) Homogenization and trend analysis of Canadian near-surface wind speeds. *Journal of Climate*, 23(5), 1209–1225.

Wang, L., Chen, W., Zhou, W. and Huang, R.H. (2009) Interannual variations of East Asian trough axis at 500 hPa and its association with the East Asian winter monsoon pathway. *Journal of Climate*, 22(3), 600–614.

Wang, X.L. (2008) Penalized maximal *F*-test for detecting undocumented mean-shifts without trend-change. *Journal of Atmospheric and Oceanic Technolgoy*, 25(3), 368–384.

Wang, X.L. and Feng, Y. (2013) *RHtestV4 User Manual*. Toronto, ON: Climate Research Division, Science and Technology Branch, Environment Canada, 28 pp.

Wang, X.L., Wen, Q.H. and Wu, Y. (2007) Penalized maximal *t* test for detecting undocumented mean change in climate data series. *Journal of Atmospheric and Oceanic Technology*, 46(6), 916–931.

WMO. (2017) *Greenhouse Gas Bulletin*. Geneva: World Meteorological Organization.

Wu, D.X., Li, Q., Lin, X.P. and Bao, X.W. (2005) The characteristics of the Bohai Sea SST anomaly interannual variability during 1990–1999. *Journal of Ocean University of China*, 35(2), 173–176 (in Chinese with English abstract).

Xu, W.H., Li, Q.X., Wang, X.L., Yang, S., Cao, L.J. and Feng, Y. (2013) Homogenization of Chinese daily surface air temperature and analysis of trends in the extreme temperature indices. *Journal of Geophysical Research*, 118(17), 9708–9720.

Yan, J.Y. and Li, J.L. (1997) Temperature changes in the East China Sea and its adjacent areas for a hundred years. *Acta Meteorologica Sinica*, 19(6), 121–127 (in Chinese with English abstract).

Yeh, S.W. and Kim, C.H. (2010) Recent warming in the Yellow/East China Sea during winter and the associated atmospheric circulation. *Continental Shelf Research*, 30(13), 1428–1434.

You, Q.L., Kang, S.C., Aguilar, E., Pepin, N., Flügel, W.A., Yan, Y.P., Xu, Y., Zhang, Y. and Huang, J. (2011) Changes in daily climate extremes in China and their connection to the large scale atmospheric circulation during 1961–2003. *Climate Dynamics*, 36, 2399–2417.

You, Q.L., Ren, G.Y., Fraedrich, K., Kang, S., Ren, Y.Y. and Wang, P. L. (2013) Winter temperature extremes in China and their possible causes. *International Journal of Climatology*, 33(6), 1444–1455.

Zhang, A.Y., Ren, G.Y., Zhou, J.X., Ren, Y.Y. and Tang, G.L. (2010) Urbanization effect on surface air temperature trends over China. *Acta Meteorologica Sinica*, 68(6), 957–966.

Zhang, L., Ren, G.Y., Ren, Y.Y. and Zhou, Q.Y. (2014) Effect of data homogenization on estimate of temperature trend: a case of Huairou station in Beijing Municipality. *Theoretical and Applied Climatology*, 115(34), 365–373.

Zhang, W. (1991) Automatic observation system at Xiaomaidao Ocean station. *Ocean Technology*, 10(1), 55–61 (in Chinese with English abstract).

Zhu, Y.N., Cao, L.J., Tang, G.L. and Zhou, Z.J. (2015) Homogenization of surface relative humidity over China. *Climate Change Research*, 11(6), 379–386 (in Chinese with English abstract).

How to cite this article: Li Y, Mu L, Wang Q, Ren G, You Q. High-quality sea surface temperature measurements along coast of the Bohai and Yellow Seas in China and their long-term trends during 1960–2012. *Int J Climatol*. 2020;40:63–76. https://doi.org/10.1002/joc.6194